



In the format provided by the authors and unedited.

# Localization of microscale devices in vivo using addressable transmitters operated as magnetic spins



Manuel Monge <sup>1</sup>, Audrey Lee-Gosselin<sup>2</sup>, Mikhail G. Shapiro <sup>2\*</sup> and Azita Emami<sup>1\*</sup>

---

<sup>1</sup>Division of Engineering and Applied Sciences, California Institute of Technology, Pasadena, CA 91125, USA. <sup>2</sup>Division of Chemistry and Chemical Engineering, California Institute of Technology, Pasadena, CA 91125, USA. \*e-mail: [mikhail@caltech.edu](mailto:mikhail@caltech.edu); [azita@caltech.edu](mailto:azita@caltech.edu)

In the format provided by the authors and unedited.

# Localization of microscale devices in vivo using addressable transmitters operated as magnetic spins

Manuel Monge <sup>1</sup>, Audrey Lee-Gosselin<sup>2</sup>, Mikhail G. Shapiro <sup>2\*</sup> and Azita Emami<sup>1\*</sup>

---

<sup>1</sup>Division of Engineering and Applied Sciences, California Institute of Technology, Pasadena, CA, 91125, USA. <sup>2</sup>Division of Chemistry and Chemical Engineering, California Institute of Technology, Pasadena, CA, 91125, USA. \*e-mail: [mikhail@caltech.edu](mailto:mikhail@caltech.edu); [azita@caltech.edu](mailto:azita@caltech.edu)

In the format provided by the authors and unedited.

# Localization of microscale devices in vivo using addressable transmitters operated as magnetic spins

Manuel **Monge**<sup>1</sup>, Audrey **Lee-Gosselin**<sup>2</sup>, Mikhail G. **Shapiro**<sup>2\*</sup> and Azita **Emami**<sup>1\*</sup>

<sup>1</sup>Division of Engineering and Applied Sciences, California Institute of Technology, Pasadena, CA, 91125, USA. <sup>2</sup>Division of Chemistry and Chemical Engineering, California Institute of Technology, Pasadena, CA, 91125, USA. \*e-mail: [mikhail@caltech.edu](mailto:mikhail@caltech.edu); [azita@caltech.edu](mailto:azita@caltech.edu)

## SUPPLEMENTARY MATERIAL

### Localization of Microscale Devices *In Vivo* using Addressable Transmitters Operated as Magnetic Spins

Manuel Monge<sup>1</sup>, Audrey Lee-Gosselin<sup>2</sup>, Mikhail G. Shapiro<sup>2\*</sup>, Azita Emami<sup>1\*</sup>

<sup>1</sup>Division of Engineering and Applied Sciences,

<sup>2</sup>Division of Chemistry and Chemical Engineering

California Institute of Technology, Pasadena, CA, USA 91125

\*Correspondence: [azita@caltech.edu](mailto:azita@caltech.edu) or [mikhail@caltech.edu](mailto:mikhail@caltech.edu)

I. Theoretical Spatial Resolution

II. Angular Misalignment

Supplementary Figure S1 – ATOMS localization

Supplementary Figure S2 – 3-D localization schemes

Supplementary Figure S3 – Compensation scheme for angular misalignment

## I. THEORETICAL SPATIAL RESOLUTION

Consider an ATOMS device inside a body in a magnetic field profile  $B_Z = g(x)$  as shown in **Figure S1**. The location of ATOMS can be estimated by mapping the magnetic field back in space according to

$$\hat{x} = g^{-1} \left( \frac{\Delta f + \Delta f_0}{\gamma_{ATOMS}} \right), \quad (S1)$$

where  $g^{-1}$  is the inverse function of  $B_Z$ ,  $\Delta f$  is the frequency shift,  $\Delta f_0$  is the frequency shift offset, and  $\gamma_{ATOMS}$  is the gyromagnetic ratio of the ATOMS device. To calculate the spatial resolution  $\Delta x$  for frequency encoding, we first take the derivative of Eq. (S1) and, using the inverse function theorem, we obtain

$$\hat{x}' = \frac{1}{g'(x)} = \frac{1}{G_Z}, \quad (S2)$$

where  $G_Z = dB_Z/dx$  is the magnetic field gradient of  $B_Z$ . The spatial resolution is then given by

$$\Delta x = \frac{\Delta f_{\min}}{\gamma_{ATOMS} G_Z}, \quad (S3)$$

where we define  $\Delta f_{\min} = 2\sigma_f$  as the minimum detectable frequency shift.  $\sigma_f$  is the standard deviation of the oscillation frequency and is defined as

$$\sigma_f = \sqrt{(\gamma_{ATOMS} \sigma_{MS})^2 + \sigma_{PN}^2}, \quad (S4)$$

where  $\sigma_{MS}$  is the magnetic sensor noise and  $\sigma_{PN}$  is the standard deviation of the oscillator's phase noise. Since the dominant noise source close to the oscillation frequency is flicker noise, the phase noise profile of the oscillator  $S_\phi(\omega)$  can be approximated by a Gaussian profile in this region<sup>1-3</sup>. Thus, its standard deviation can be estimated by  $\sigma_{PN} \approx FWHM_{S_\phi}/2.355$ , where  $FWHM_{S_\phi}$  is the full width at half maximum or 3-dB bandwidth of  $S_\phi(\omega)$ .

## II. ANGULAR MISALIGNMENT

In the case of an angular misalignment of  $\theta^\circ$  degrees between  $B_Z$  and an ATOMS device (**Fig. S3a**), the measured magnetic field will be proportional to the projection of  $B_Z$  into the plane orthogonal to the device (i.e.,  $B_Z \cos \theta$ ), and can reduce the accuracy of the system. The polar angle  $\xi$ , in contrast, will not affect the resolution because the device only measures the orthogonal magnetic field. To overcome this limitation, we devise the following method which can be applied to frequency and phase encoding. We add an extra step in the pulse sequence where a uniform magnetic field  $B_C$  is applied to measure a

28 correction factor and correctly estimate  $B_{G_Z}$ , the local magnetic field at the device's location generated by  
 29 the field gradient  $G_Z$ .

30 **Figure S3b** shows the pulse sequence for localization of a single ATOMS device with angular  
 31 misalignment. We first apply the known field  $B_C$ . In this case, the ATOMS device measures  $B_{MC} =$   
 32  $B_C \cos \theta$ , which is estimated from the measured frequency shift by

$$33 \quad B_{MC} = \frac{\Delta f_{MC}}{\gamma_{ATOMS}}, \quad (S5)$$

34 where  $\Delta f_{MC}$  is the frequency shift due to  $B_{MC}$ . Then, the angular misalignment can be estimated by

$$35 \quad \theta = \cos^{-1} \left( \frac{B_{MC}}{B_C} \right). \quad (S6)$$

36 Second, we apply  $G_Z$  and the chip measures  $B_{MZ} = B_{G_Z} \cos \theta$ . Similarly,  $B_{MZ}$  is estimated by

$$37 \quad B_{MZ} = \frac{\Delta f_{MZ}}{\gamma_{ATOMS}}, \quad (S7)$$

38 where  $\Delta f_{MZ}$  is the frequency shift due to  $B_{MZ}$ . Finally, combining the device's measurements  $B_{MC}$  and  
 39  $B_{MZ}$  with equations (S5) and (S7) gives

$$40 \quad \frac{B_{MZ}}{B_{MC}} = \frac{B_{G_Z} \cos \theta}{B_C \cos \theta} = \frac{\Delta f_{MZ}/\gamma_{ATOMS}}{\Delta f_{MC}/\gamma_{ATOMS}}, \quad (S8)$$

$$41 \quad B_{G_Z} = B_C \frac{\Delta f_{MZ}}{\Delta f_{MC}}. \quad (S9)$$

42 This approach allows the correct estimation of the ATOMS device's location and also enables the  
 43 estimation of its orientation as long as the local magnetic fields  $B_{MC}$  and  $B_{MZ}$  are above the noise floor of  
 44 the magnetic sensor. This means

$$45 \quad B_C \cos \theta \text{ or } B_{G_Z} \cos \theta > B_{\min}, \quad (S10)$$

46 where  $B_{\min}$  is the resolution of the magnetic sensor. Therefore, the maximum angular misalignment  $\theta_{\max}$   
 47 is given by

$$48 \quad \theta_{\max} = \cos^{-1} \left( \frac{B_{\min}}{B_{G_Z \min}} \right), \text{ with } B_{G_Z \min} < B_C, \quad (S11)$$

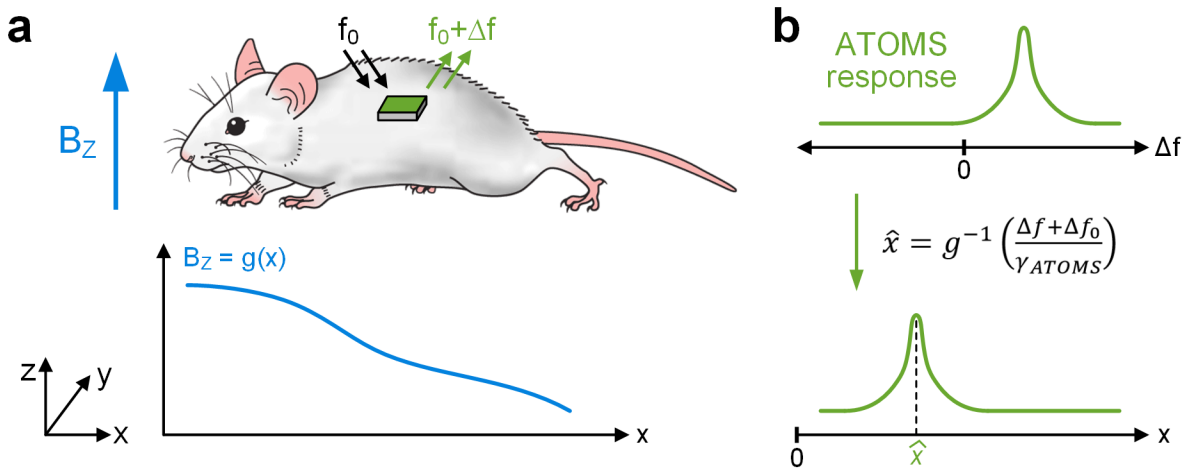
49 where  $B_{G_Z \min}$  is the minimum magnetic field generated by the field gradient  $G_Z$ .

50 For a single device,  $\Delta f_{MC}$  and  $\Delta f_{MZ}$  can be obtained in two successive acquisitions. For localization of  
 51 multiple arbitrarily arranged ATOMS devices (**Fig. S3c**), the device can calculate the alignment  
 52 correction internally (on-chip). In this scenario, both  $B_C$  and  $G_Z$  are applied consecutively so that the

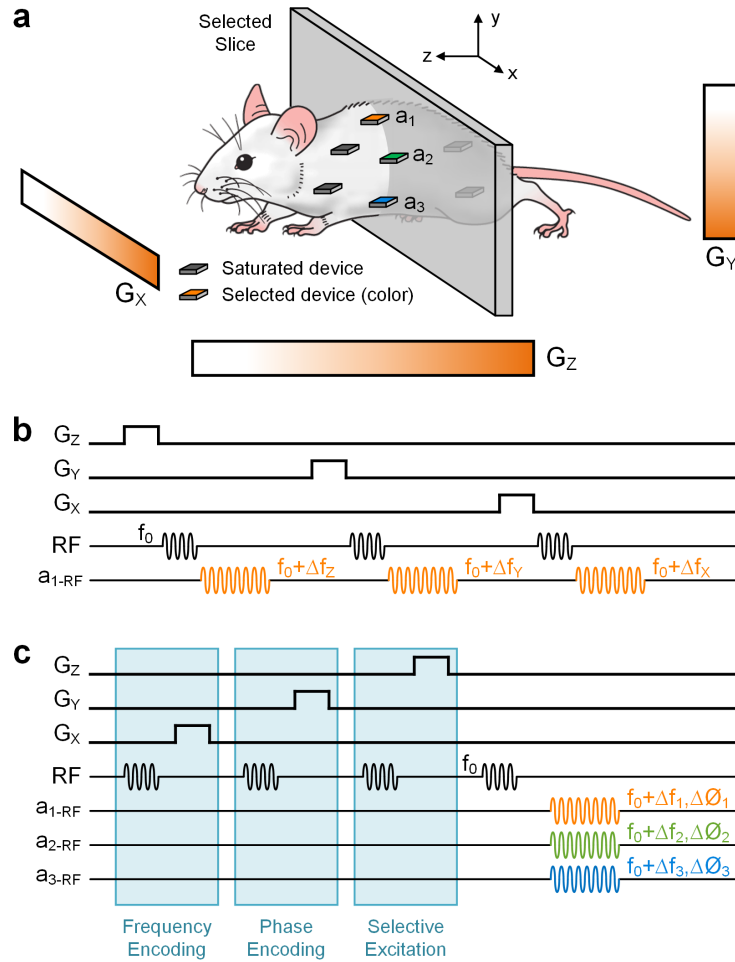
53 devices measure  $B_{MC}$  and  $B_{MZ}$ . Then, each device calculates the ratio of  $B_{MC}$  and  $B_{MZ}$  and shifts its  
 54 oscillation frequency according to

55 
$$\Delta f = \alpha \frac{B_{MZ}}{B_{MC}} \gamma_{ATOMS} = \alpha \frac{B_{GZ}}{B_C} \gamma_{ATOMS}, \quad (S12)$$

56 where  $\alpha$  is a constant pre-programmed into the device which is set by the target bandwidth utilization.  
 57 Thus, the location of each device is estimated as described above.

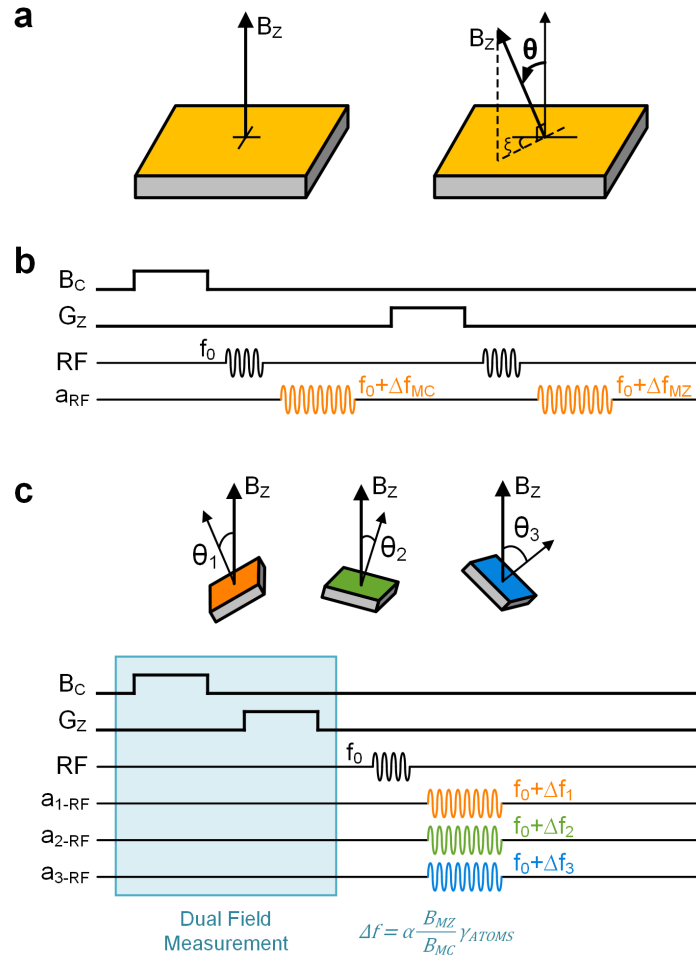


**Supplementary Figure S1 – ATOMS localization.** Illustration of the localization process of an ATOMS device inside the body of an animal or patient. (a) The ATOMS chip responds to the excitation RF signal by transmitting a signal with a frequency shift  $\Delta f$  proportional to the magnetic field generated by  $B_Z = g(x)$  at the device's location. (b) The chip's response is used to estimate its location by mapping the magnetic field back in space according to  $\Delta f$ , its gyromagnetic ratio  $\gamma_{ATOMS}$  and the inverse function  $g^{-1}$ .



**Supplementary Figure S2 – 3-D localization schemes.** (a) Illustration for 3-D localization of ATOMS devices.  $G_X$ ,  $G_Y$  and  $G_Z$  are the magnetic field gradients. (b) Pulse sequence for 3-D localization of a single device ( $a_1$ ) using only frequency encoding. The frequency shifts after each RF excitation  $\Delta f_X$ ,  $\Delta f_Y$  and  $\Delta f_Z$  are proportional to the local magnetic field generated by  $G_X$ ,  $G_Y$  and  $G_Z$ , respectively. By mapping these frequency shifts back in space, the location of  $a_1$  can be determined. (c) Pulse sequence for 3-D localization of multiple devices. ATOMS devices can be designed to expect four RF pulses before transmitting their responds. The first two pulses trigger the chips to sense the magnetic field generated by  $G_X$  and  $G_Y$ , and set  $\Delta f$  and  $\Delta \phi$ , respectively. The third pulse tells the devices to sense the field generated by  $G_Z$  and become silent during transmission if they experience a field magnitude above a certain threshold (outside the slice of interest). The final RF pulse is then used for frequency acquisition and synchronization, and to indicate devices not saturated by  $G_Z$  (selected devices  $a_1$ ,  $a_2$  and  $a_3$ ) to start transmitting according to their frequency and phase shifts ( $\Delta f_1$ ,  $\Delta f_2$ ,  $\Delta f_3$ , and  $\Delta \phi_1$ ,  $\Delta \phi_2$ ,  $\Delta \phi_3$ , respectively). These frequency and phase shifts are then mapped back in space to estimate the location of selected devices.





**Supplementary Figure S3 – Compensation scheme for angular misalignment.** (a) Illustration of angular misalignment, where  $\theta$  is the azimuthal angle and  $\xi$  is the polar angle. In this case, the ATOMS device measures  $B_Z \cos \theta$ . (b) Pulse sequence for localization of a single device with angular misalignment. An extra step in the pulse sequence is added where a uniform magnetic field  $B_C$  is applied to measure a correction factor. This factor is used to estimate the local magnetic field generated by  $G_Z$  ( $B_{G_Z}$ ) from measured frequency shifts  $\Delta f_{MC}$  and  $\Delta f_{MZ}$ , and the known field  $B_C$ . (c) Pulse sequence for localization of multiple arbitrarily aligned ATOMS devices. In this case, each device calculates the ratio of measured fields  $B_{MZ}$  and  $B_{MC}$ , and shifts its oscillation frequency in proportion to this ratio,  $\gamma_{ATOMS}$ , and the bandwidth utilization constant  $\alpha$ .

## References

1. Herzel, F. An analytical model for the power spectral density of a voltage-controlled oscillator and its analogy to the laser linewidth theory. *IEEE Trans. Circuits Syst. I Fundam. Theory Appl.* **45**, 904–908 (1998).
2. Navid, R., Lee, T. H. & Dutton, R. W. An analytical formulation of phase noise of signals with Gaussian-distributed jitter. *IEEE Trans. Circuits Syst. II Express Briefs* **52**, 149–153 (2005).
3. Chorti, A. & Brookes, M. A spectral model for RF oscillators with power-law phase noise. *IEEE Trans. Circuits Syst. I Regul. Pap.* **53**, 1989–1999 (2006).